Origin of pressure-induced anomalies in the nodal-line ferrimagnet $Mn_3Si_2Te_6$ – Supplementary Information –

Varun Venkatasubramanian,[1] Makoto Shimizu,[2] Daniel Guterding,[3] and Harald O. Jeschke[1]

[1] *Research Institute for Interdisciplinary Science, Okayama University, Okayama 700-8530, Japan*
[2] *Department of Physics, Graduate School of Science, Kyoto University, Kyoto 606-8502, Japan*
[3] *Technische Hochschule Brandenburg, Magdeburger Straße 50, 14770 Brandenburg an der Havel, Germany*

Supplementary Note 1. ADDITIONAL DFT RESULTS

In Supplementary Figs. 1 and 2, we present the structural information that is the basis for all further calculations. Lattice parameters as a function of pressure are taken from experiment and interpolated. For the trigonal $P\bar{3}1c$ phase, internal coordinates are optimized with a generic DFT+U functional in the ferromagnetic state. Relaxation in ferrimagnetic state yields very similar results.

For the monoclinic structure, we find that structure relaxation takes the internal coordinates too far away from the experimentally determined ones. Therefore, we only vary the lattice parameters as shown in Supplementary Fig. 2 and keep the internal coordinates fixed at the values of the $P = 22.3$ GPa experimental structure. The corresponding bond lengths are shown in Fig. 3.

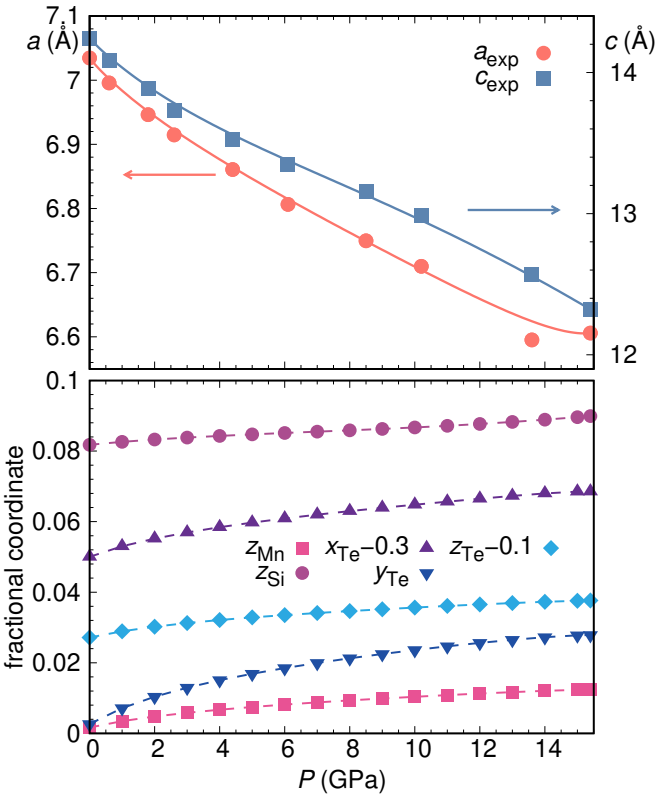

Supplementary Figure 1. Structure parameters of $Mn_3Si_2Te_6$ as a function of pressure for the $P\bar{3}1c$ space group. (a) Interpolated lattice parameters; symbols are experimental points taken from Ref. 1. Lines are smooth interpolations that were used for this study. (b) Fractional coordinates of $Mn_3Si_2Te_6$ determined by relaxation of the structures with a DFT+U functional at $U = 5$ eV in a ferromagnetic state. Dashed lines are guides to the eye.

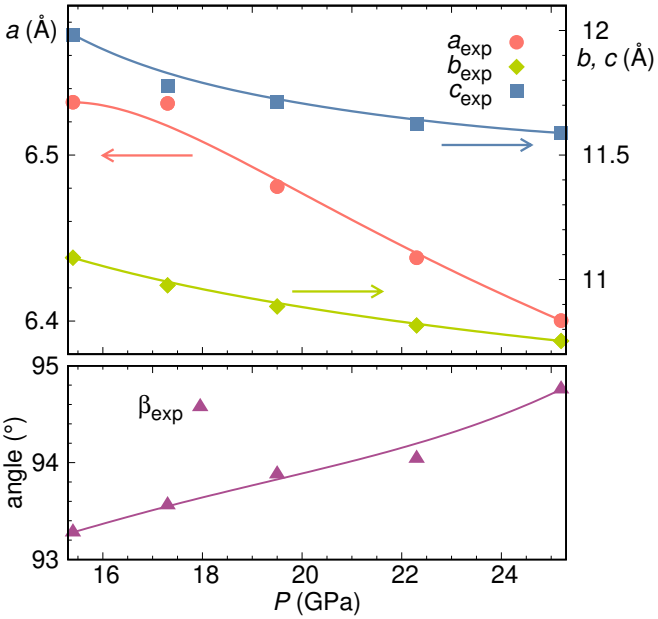

Supplementary Figure 2. Structure parameters of $Mn_3Si_2Te_6$ as a function of pressure for the $C2/c$ space group. (a) Interpolated lattice parameters and (b) monoclinic β angle; symbols are experimental points taken from Ref. 1. Lines are smooth interpolations that were used for this study.

In Supplementary Figs. 4, 5 and 6 we show DFT plus spin-orbit coupling (DFT+SOC) electronic band structures with atomic weights at pressures $P = 0$ GPa, $P = 7$ GPa and $P = 13$ GPa. These correspond to the low-pressure trigonal phase, which has an insulating ferrimagnetic ground state with spins oriented in the ab plane. The subplots show the band structure as a function of the spin quantization axis. For an orientation along the c axis (hard axis) (see Supplementary Fig. 6), the insulator to metal transition happens below the critical pressure of $P_c = 15.4$ GPa. This is reminiscent of the field-driven insulator to metal transition in $Mn_3Si_2Te_6$. [2]

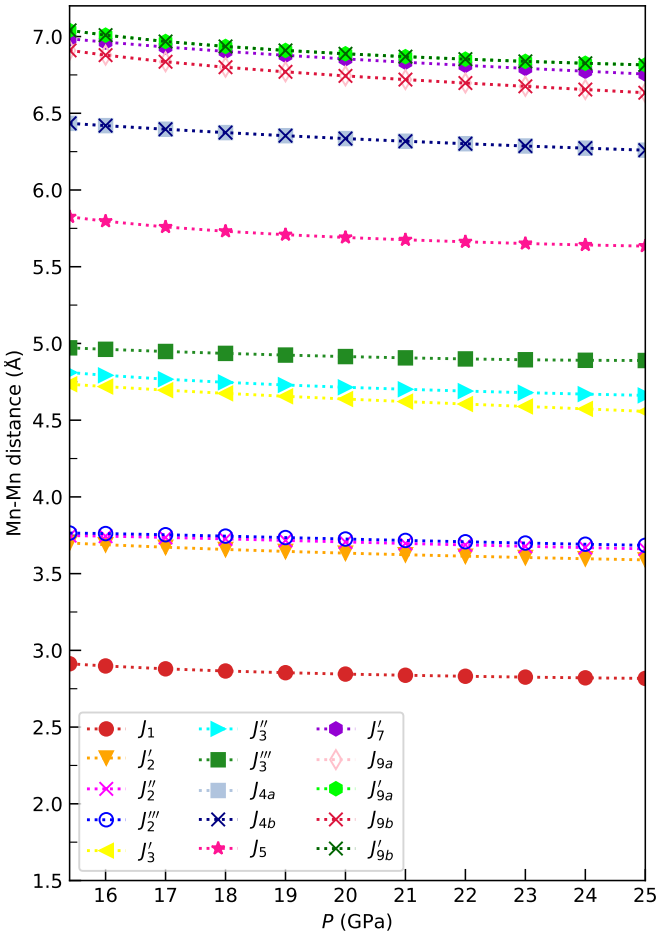

Supplementary Figure 3. Evolution of the nearest neighbour Mn-Mn distances as a function of pressure for the monoclinic structures of $Mn_3Si_2Te_6$.

Supplementary Note 2. ADDITIONAL MONTE CARLO RESULTS

In Supplementary Fig. 7 we show how the choice of U affects the ordering temperature. For this we ran classical Monte Carlo calculations for the Hamiltonians of trigonal $Mn_3Si_2Te_6$ at $P = 0$ GPa at five additional values of U. The resulting ground state is always the same ferrimagnetic order. The transition temperature changes linearly with U as shown in Supplementary Fig. 7, decreasing from 69 K at $U = 4$ eV to 37 K at $U = 6$ eV. This means that using $U = 4$ eV or $U = 4.5$ eV instead of the value $U = 4.2$ eV that we chose for our study would only have the effect of shifting transition temperatures up or down by a few Kelvin. Therefore, our results are robust and no qualitatively different results are to be expected for other reasonable choices of U.

Supplementary Fig. 8 shows the specific heat of $Mn_3Si_2Te_6$ at ambient pressure, calculated with four different system sizes. We find that the peak in the specific heat has little system size dependence. The ordering temperature can be reliably determined from the $8 \times 8 \times 8$ system (3072 spins),

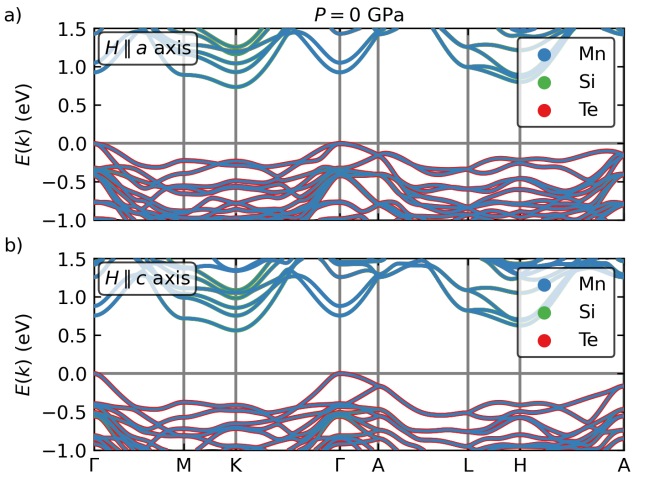

Supplementary Figure 4. DFT+SOC band structure at $P = 0$ GPa with atomic weights and in the ferrimagnetic ground state. In (a) the spins are oriented along the a axis, in (b) spins are oriented along the c axis.

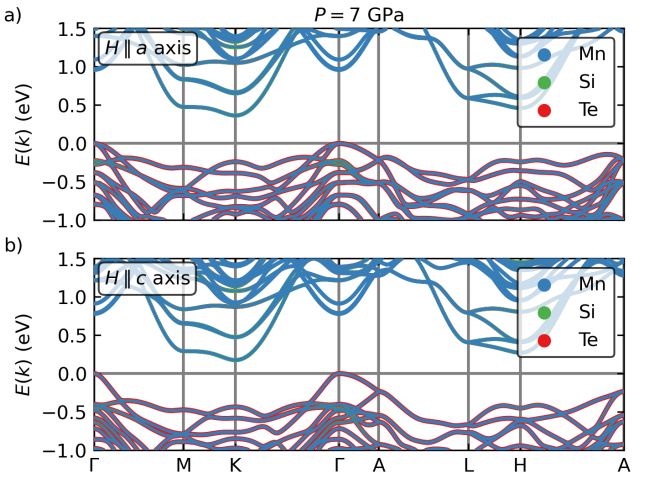

Supplementary Figure 5. DFT+SOC band structure at $P = 7$ GPa with atomic weights and in the ferrimagnetic ground state. In (a) the spins are oriented along the a axis, in (b) spins are oriented along the c axis.

and we perform all subsequent calculations with this system size.

We present the calculated specific heat for trigonal and monoclinic structures of $Mn_3Si_2Te_6$ in Supplementary Figures 9 and 10. We use the position of the maxima to determine the ferrimagnetic ordering temperatures plotted in Figure 5 of the main text.

In Supplementary Figs. 11 and 12 we also show the magnetization curves as a function of temperature for all pressure values we considered. The magnetization value 1/3 corresponds to the ferrimagnetic state where Mn trimers are in an up-down-up state and all trimers in the lattice are ferromagnetically ordered. In the monoclinic phase, some

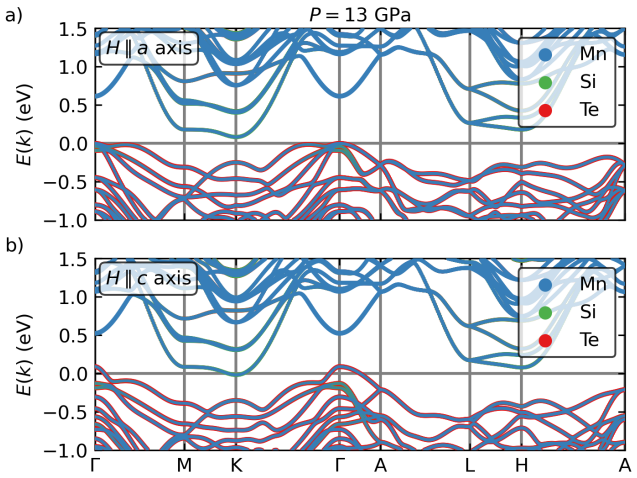

Supplementary Figure 6. DFT+SOC band structure at $P = 13$ GPa with atomic weights and in the ferrimagnetic ground state. In (a) the spins are oriented along the a axis, in (b) spins are oriented along the c axis.

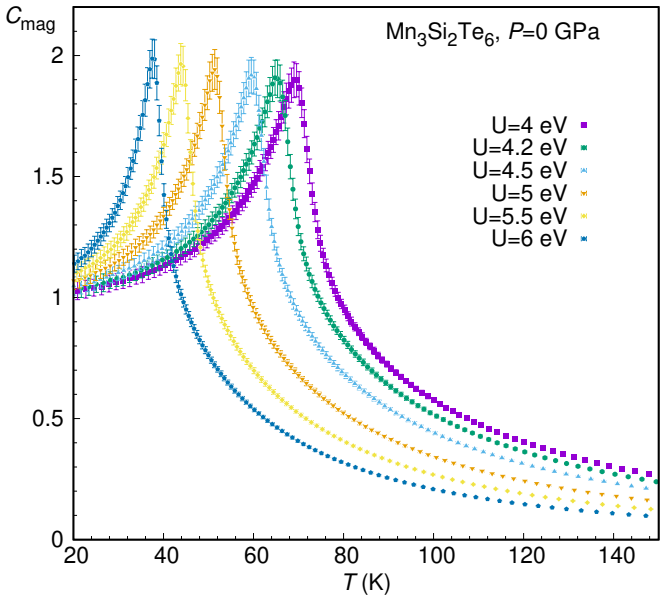

Supplementary Figure 7. Specific heat for the trigonal $P\bar{3}1c$ structure of $Mn_3Si_2Te_6$ at $P = 0$ GPa for different values of the on-site repulsion U.

frustration in the Hamiltonian leads to a small modulation of the ferrimagnetic state so that the total magnetization for example for 15.4, 16 and 17 GPa does not reach the full 1/3.

Supplementary Note 3. REGULARIZATION OF HEISENBERG COUPLING ESTIMATES

In the main text we use L_1-regularized estimates for the isotropic Heisenberg parameters. We choose a regularization parameter $\alpha = 0.04$, which leads to marginally higher mean-squared error (MSE) compared to the ordinary least squares (OLS) solution for each pressure, but delivers stabilized Heisenberg parameter estimates. The so-called elbow plot for the MSE as a function of the regularization strength α is shown in Supplementary Fig. 13.

Supplementary Fig. 14 shows the energy differences w.r.t. the DFT energies per Mn for each of the 100 spin configurations and each pressure point.

In Supplementary Fig. 15 we show the isotropic Heisenberg parameters and the mean-squared error as a function of pressure for different values of regularization strength.

The critical temperature T_C without any regularization on the isotropic Heisenberg couplings is shown in Supplementary Fig. 16. Although the results in the high-pressure mon-

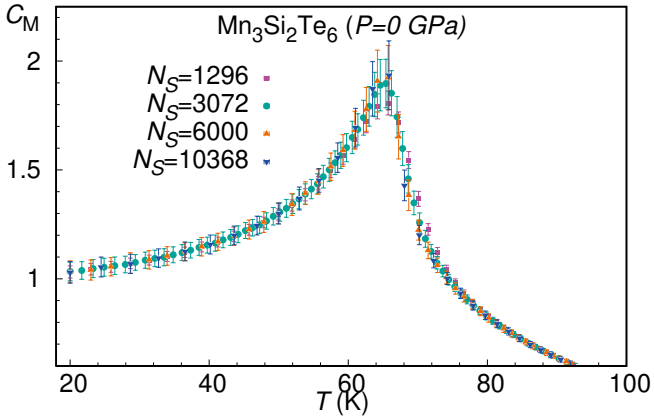

Supplementary Figure 8. Specific heat for the trigonal $P\bar{3}1c$ structure of $Mn_3Si_2Te_6$ at $P = 0$ GPa for different system sizes ($6 \times 6 \times 6$, $8 \times 8 \times 8$, $10 \times 10 \times 10$ and $12 \times 12 \times 12$).

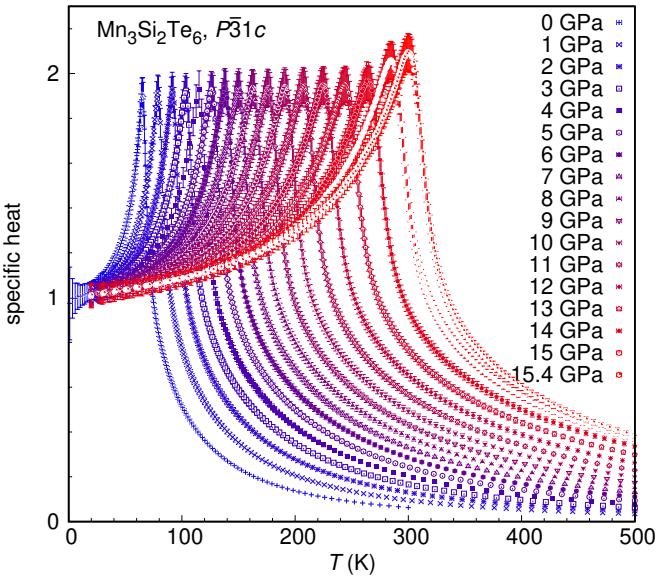

Supplementary Figure 9. Specific heat for the trigonal $P\bar{3}1c$ structure of $Mn_3Si_2Te_6$. Pressures range from $P = 0$ to $P = 15.4$ GPa.

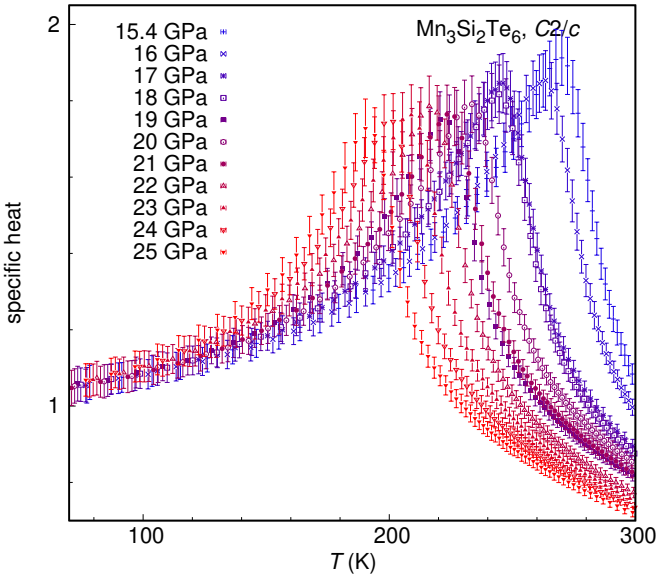

Supplementary Figure 10. Specific heat for the monoclinic $C2/c$ structure of $Mn_3Si_2Te_6$. Pressures range from $P = 15.4$ GPa to $P = 25$ GPa.

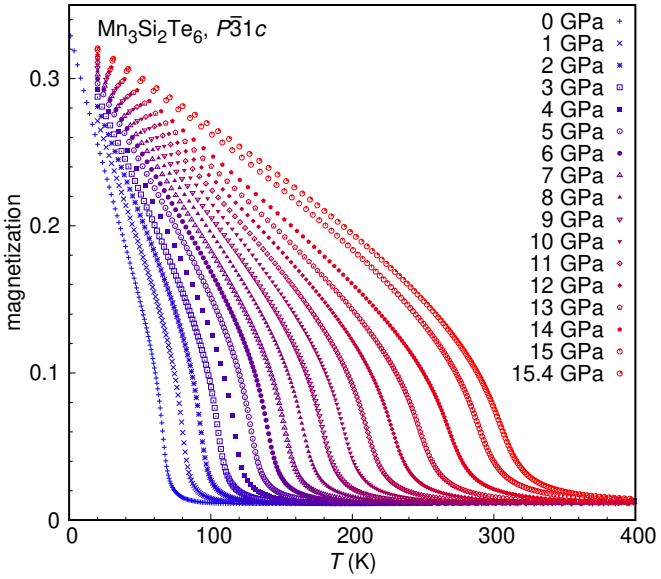

Supplementary Figure 11. Absolute value of the unit cell magnetization for the $P\bar{3}1c$ structure of $Mn_3Si_2Te_6$. Pressures range from $P = 0$ to $P = 15.4$ GPa. The value $1/3$ corresponds to the ferrimagnetic state.

oclinic phase qualitatively agree with experiment, some regularization is needed to remove some spurious frustration due to overfitting the DFT energies.

In Supplementary Fig. 17 we also show MSE and coefficients as a function of the regularization strength for $P = 15.4$ GPa.

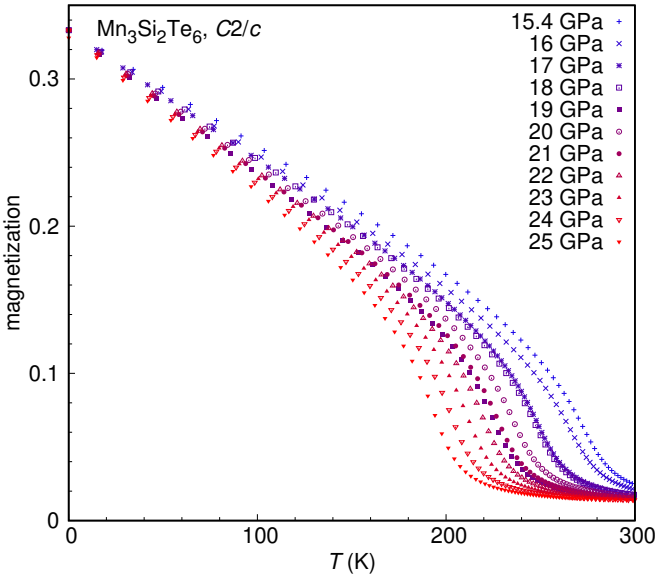

Supplementary Figure 12. Absolute value of the unit cell magnetization for the $C2/c$ structure of $Mn_3Si_2Te_6$. Pressures range from $P = 15.4$ GPa to $P = 25$ GPa. The value $1/3$ corresponds to the ferrimagnetic state.

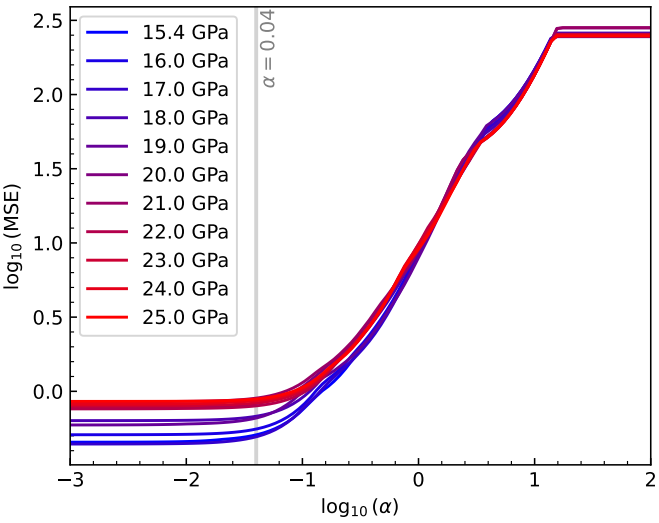

Supplementary Figure 13. Mean squared error (MSE) of isotropic Heisenberg exchange couplings in the monoclinic phase w.r.t. the DFT energies for each pressure as a function of the L_1 regularization parameter α. The grey vertical line marks the so-called elbow of the error plot, which we use to select the optimal regularization parameter $\alpha = 0.04$.

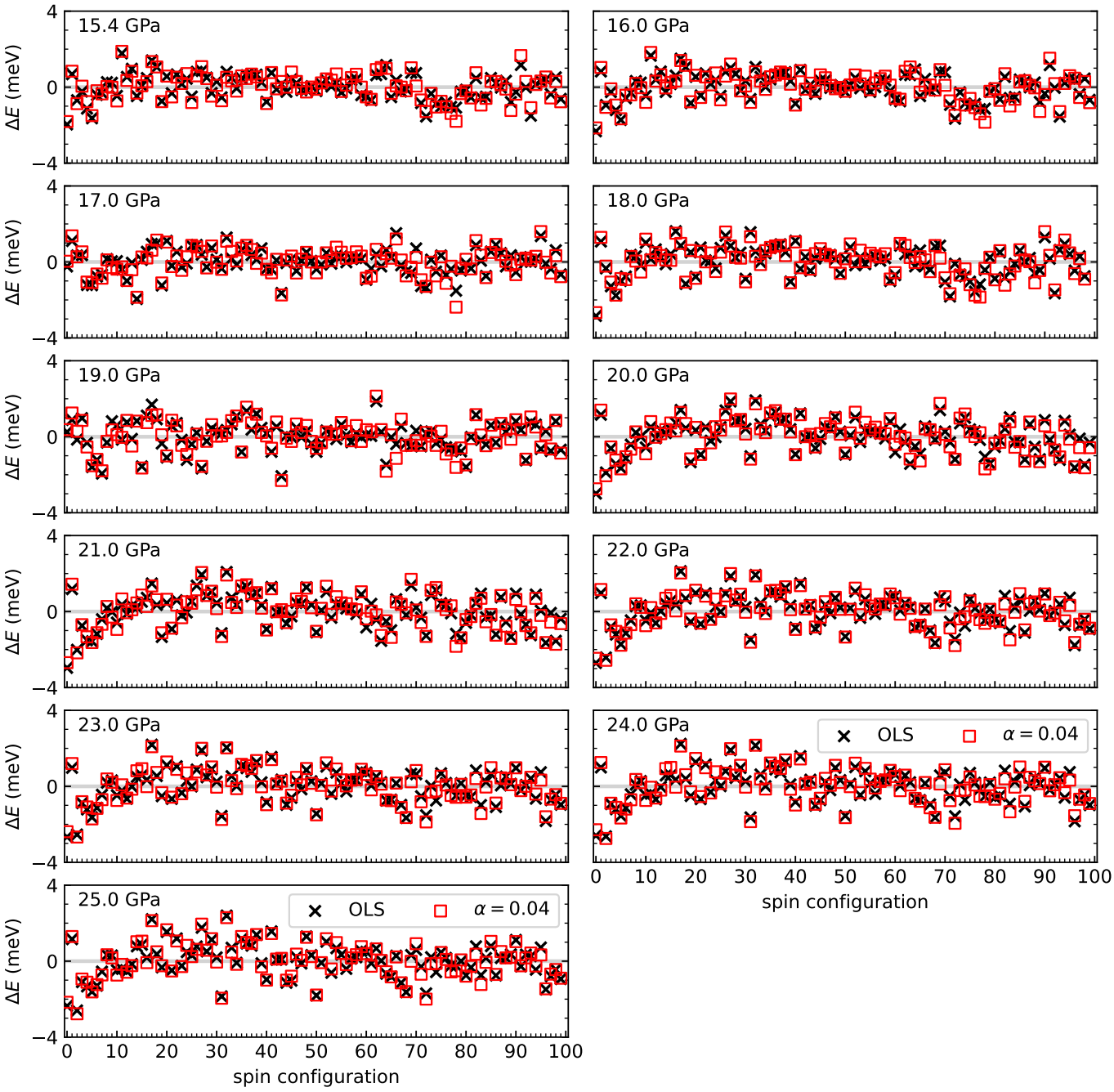

Supplementary Figure 14. Energy errors per Mn of linear models with respect to the DFT energies. OLS denotes the ordinary least-squares solution, while $\alpha = 0.04$ denotes the L_1-regularized solution.

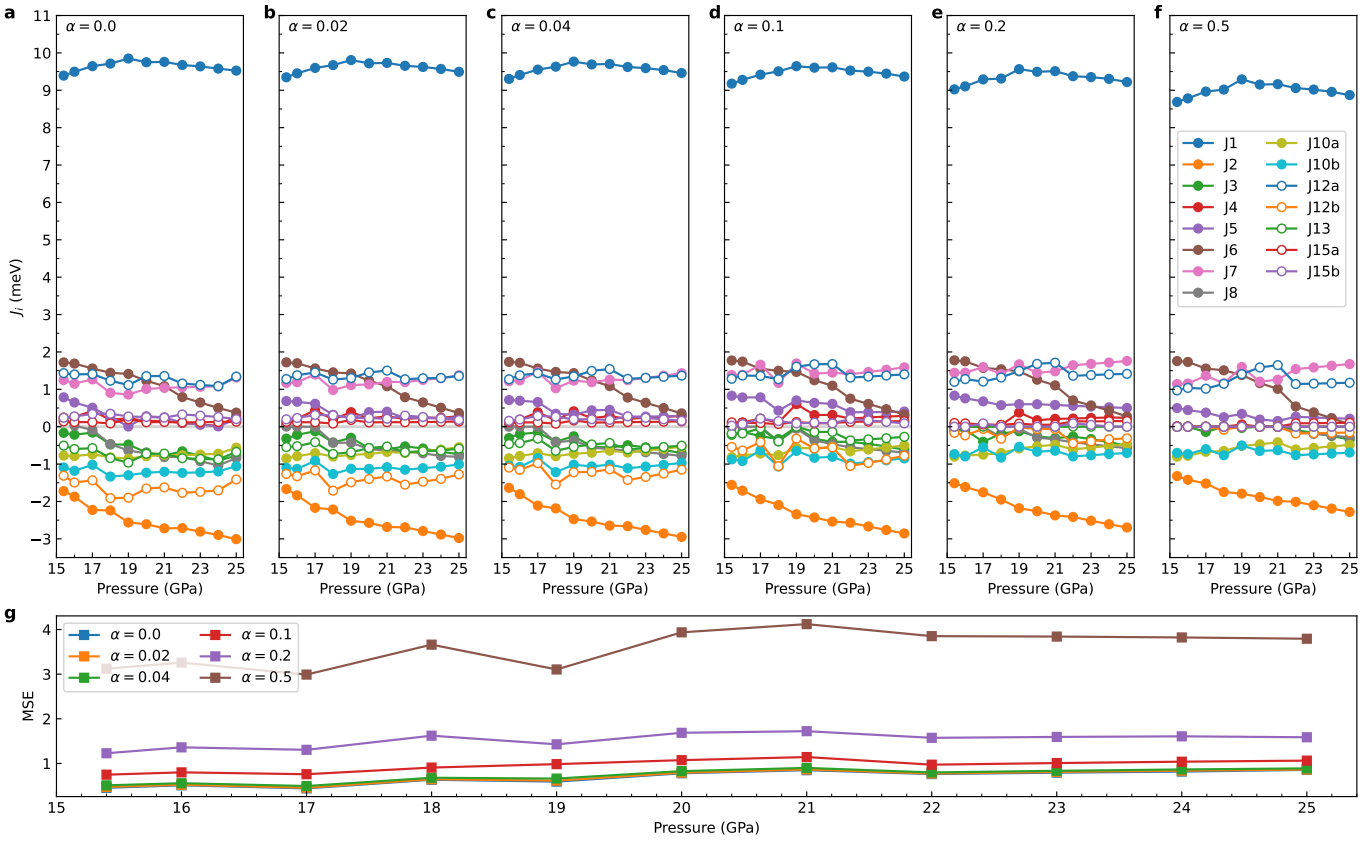

Supplementary Figure 15. Overview of **a** to **f** isotropic Heisenberg couplings and **g** the mean-squared error (MSE) in the monoclinic phase as a function of the L_1 regularization parameter α.

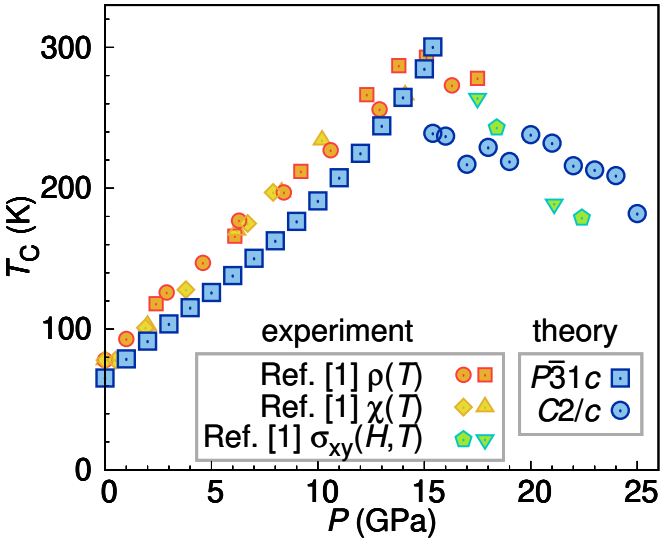

Supplementary Figure 16. Predicted ferrimagnetic ordering temperatures (blue symbols) for $Mn_3Si_2Te_6$ as function of pressure, compared to the experimental data from Ref. 1 (yellow, orange and green symbols). The theoretical prediction is based on the isotropic Hamiltonian determined from the DFT energy mapping without regularization.

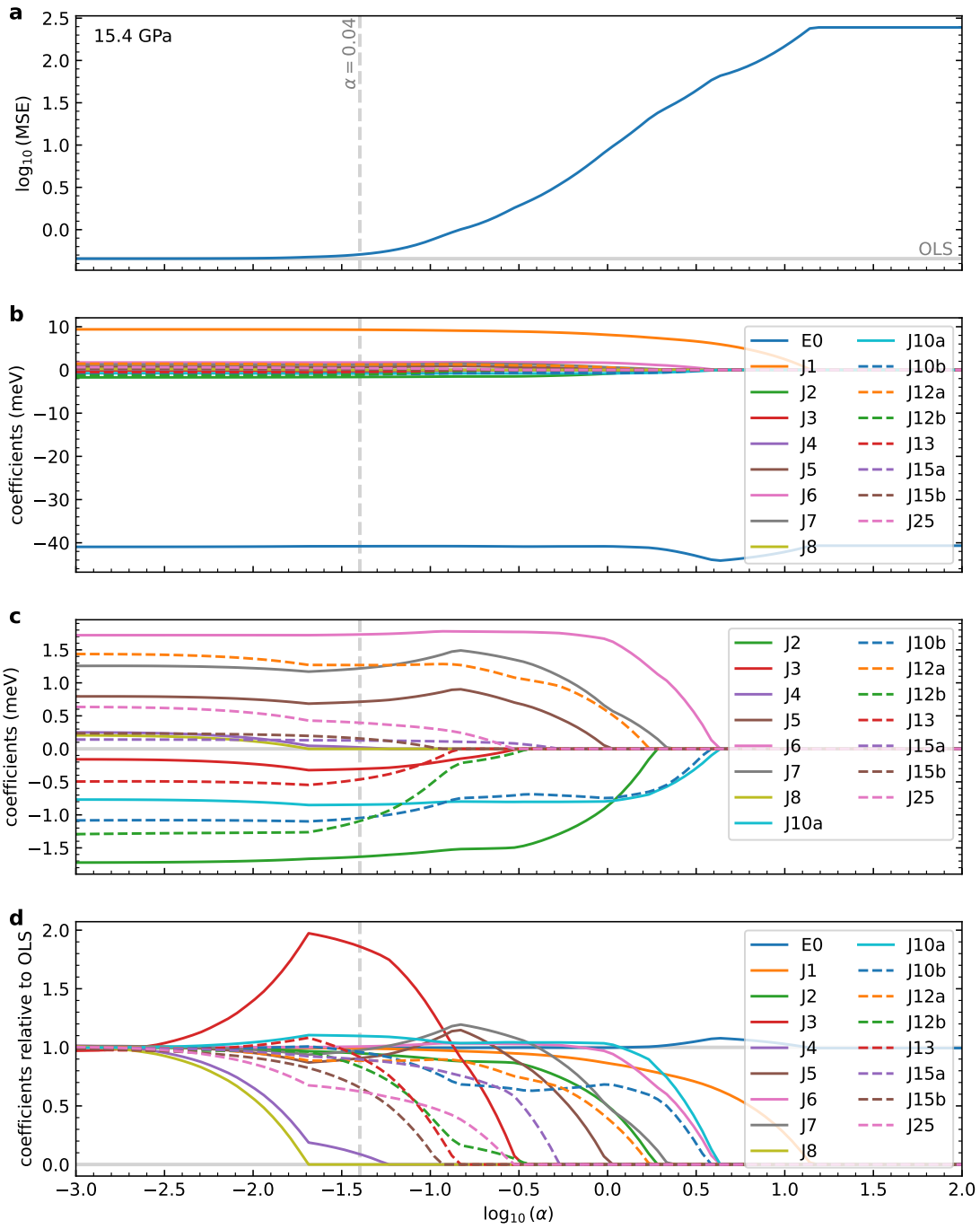

Supplementary Figure 17. (a) Mean squared error, (b, c) coefficients and (d) coefficient values relative to the un-regularized OLS values as a function of the L_1 regularization parameter α for $P = 15.4$ GPa.

[1] R. A. Susilo, C. I. Kwon, Y. Lee, N. P. Salke, C. De, J. Seo, B. Kang, R. J. Hemley, P. Dalladay-Simpson, Z. Wang, D. Y. Kim, K. Kim, S.-W. Cheong, H. W. Yeom, K. H. Kim, and J. S. Kim, High-temperature concomitant metal-insulator and spin-reorientation transitions in a compressed nodal-line ferrimagnet $Mn_3Si_2Te_6$, Nat. Commun. **15**, 3998 (2024).

[2] Y. Gu, K. A. Smith, A. Saha, C. De, C.-j. Won, Y. Zhang, L.-F. Lin, S.-W. Cheong, K. Haule, M. Ozerov, T. Birol, C. Homes, E. Dagotto, and J. L. Musfeldt, Unconventional insulator-to-metal phase transition in $Mn_3Si_2Te_6$, Nat. Commun. **15**, 8104 (2024).